



Optical beam transport to a remote location for low jitter pump-probe experiments with a free electron laser

P. Cinquegrana, S. Cleva, A. Demidovich, G. Gaio, R. Ivanov, G. Kurdi, I. Nikolov, P. Sigalotti, and M. B. Danailov*

Elettra-Sincrotrone Trieste, SS 14 - km 163.5, 34149, Basovizza Trieste, Italy

(Received 14 January 2014; published 7 April 2014)

In this paper we propose a scheme that allows a strong reduction of the timing jitter between the pulses of a free electron laser (FEL) and external laser pulses delivered simultaneously at the FEL experimental stations for pump-probe-type experiments. The technique, applicable to all seeding-based FEL schemes, relies on the free-space optical transport of a portion of the seed laser pulse from its optical table to the experimental stations. The results presented here demonstrate that a carefully designed laser beam transport, incorporating also a transverse beam position stabilization, allows one to keep the timing fluctuations, added by as much as 150 m of free space propagation and a number of beam folding mirrors, to less than 4 femtoseconds rms. By its nature our scheme removes the major common timing jitter sources, so the overall jitter in pump-probe measurements done in this way will be below 10 fs (with a margin to be lowered to below 5 fs), much better than the best results reported previously in the literature amounting to 33 fs rms.

DOI: [10.1103/PhysRevSTAB.17.040702](https://doi.org/10.1103/PhysRevSTAB.17.040702)

PACS numbers: 41.60.Cr, 42.55.Vc, 78.47.J-

I. INTRODUCTION

In the past few years free electron lasers (FELs) opened exciting opportunities for new discoveries using high-brightness tunable light pulses in the extreme UV (EUV) and x-ray spectral regions [1,2]. FELs generate ultrashort pulses of duration in the 1–100 fs range which are an ideal for time resolved experiment, aimed at revealing fundamental physical phenomena in this time scale [3,4]. A significant fraction of the FEL based time resolved measurements uses the FEL pulse in combination with a pulse generated from an external laser, which provides the freedom to choose the pump or probe wavelength anywhere from soft x ray to THz. In this class of pump-probe experiments the pulses are generated by two different sources so one of the main challenges is to keep the fluctuations of their relative arrival time at the sample (referred to as “timing jitter”) as low as possible.

While two ultrafast laser oscillators can be locked to each other with a very low timing jitter (reports of subfemtosecond jitter level can be found in literature in the past decade [5,6]), the synchronization of an external laser to the FEL pulses arriving at the experimental chambers in an FEL facility involves a complex chain of subsystems. It is affected by various sources of fluctuations and noise which typically

result in overall timing jitter exceeding 100 fs rms [7,8]. A very recent result obtained at the FLASH FEL indicates that by an extremely careful design of all subsystems this value can be improved and a relative timing jitter of 33 fs has been reported [9]. Even such a jitter level is not sufficiently small for the study of many ultrafast processes. One route to overcome the problem is to implement a shot-to-shot jitter measurement which allows subsequent data postprocessing to be done. An extensive effort has been dedicated to this approach and important progress has been made in the past years [8,10]. It is clear, however, that data postprocessing does not fully solve the problem: the presence of a timing jitter comparable to the time constants of the studied physical phenomena reduces the amount of useful shots and could make very difficult the observation and optimization of the signal in complex experiments. Therefore the study of possible techniques for reducing the timing jitter of the external laser pulses is of extreme importance for both FEL and the ultrafast physics community.

Here we demonstrate, for the first time to our knowledge, that in seeded free electron laser facilities [11,12] there is an alternative root for providing external laser pulses with drastically reduced timing jitter. The scheme relies on transporting a portion of the seed laser light to the user stations for pump-probe measurements. Due to the intrinsic synchronization of the FEL pulse with the seed laser pulse, the only source of timing jitter in this case is the optical beam transport of the seed laser pulse to the pump-probe station. The results presented here show that even over a distance of 150 m (typical for FEL facilities of this type) a carefully designed optical beam transport adds a timing jitter of below 5 fs rms.

*Corresponding author.
miltcho.danailov@elettra.eu

Published by the American Physical Society under the terms of the Creative Commons Attribution 3.0 License. Further distribution of this work must maintain attribution to the author(s) and the published article's title, journal citation, and DOI.

II. DESCRIPTION OF THE BASIC SCHEME

Extreme UV (EUV) and x-ray free electron laser facilities have so far implemented two main FEL schemes with a general layout that is very similar, as shown schematically on Fig. 1. In both cases, an electron bunch is generated by a radiofrequency (rf) photoinjector (also called rf gun) via photo effect by a laser pulse impinging on a metal (or semiconductor) photocathode. The electron bunch of typical initial length of about 10 ps is then accelerated in a linear accelerator (LINAC) to an energy from 500 eV to several GeV depending on the desired emission wavelength of the FEL. The accelerated bunch is compressed to a few hundred fs and then sent to an undulator chain where the FEL pulse is generated. In the scheme called self-amplified spontaneous emission (SASE), the FEL radiation starts from shot noise generated by the accelerated electron bunch in the first undulator. Upon propagation in the properly tuned undulator chain a portion of this radiation undergoes amplification and after a sufficient undulator length reaches saturation and can deliver a high energy (mJ range) x-ray pulse. The time of emission of the latter is determined by the time of arrival of the electron bunch at the undulators and therefore is subject to the timing jitter accumulated by the bunch during its generation, acceleration and transport. It may also be affected by shot-to-shot fluctuations of the shape and current of the bunch.

In the second scheme, called seeded FEL, instead of starting from a noise, a coherent “seed” pulse is provided by an external laser (further on called seed laser, SL). Due to the interaction of the seed laser pulse and the electron bunch, the FEL action in this scheme gives rise to a highly coherent FEL radiation at the seed wavelength or one of its harmonics [11,13,14]. One of the main schemes for implementing FEL seeding is called high gain harmonic generation (HG); it relies on high power seed pulses at a wavelength that is an integer multiple of the desired FEL wavelength [13]. In this scheme the seed pulses meet the accelerated electrons in a short, so-called modulator

undulator, tuned at the seed pulse wavelength and the interaction induces energy modulation of the electrons (so-called “bunching”). In a short dispersive section the energy modulation is converted into a spatial charge modulation; the bunch propagates further in a chain of undulators tuned at the desired harmonic of the seed laser wavelength and as a result a highly coherent pulse at the x-ray wavelength is emitted. It is important to note here that the exact time of emission of the FEL pulse is determined (with an accuracy of below 1 fs) by the temporal position of the peak of the seed pulse. This feature remains true also for the other seeding technique, called direct seeding, where the FEL is seed directly at its emission wavelength. The results presented here will refer to the HG seeding scheme implemented at the FERMI FEL [11,12], however the proposed technique is fully applicable also to the direct seeding scheme.

In order to successfully operate the FEL facility, there is the need for a tight synchronization of the different subsystems to a common reference signal. This is typically obtained by distributing a low phase noise time reference signal (see Fig. 1) over high stability fiber links to the subsystems along the e-bunch path. Each of the local systems is then synchronized to the timing signal by using phase-locked loops (PLL) acting on a local oscillator.

As mentioned above, a large fraction of the time-resolved measurements by the FEL involve the use of an external laser pulse which should ideally arrive at the sample with a perfectly defined time delay (i.e., negligible timing jitter) with respect to the FEL pulse. Some of the main sources of the FEL-to-external laser timing jitter in the SASE scheme are: (i) the noise present in the distributed reference signal; (ii) the nonperfect synchronization of the ultrafast lasers [photoinjector laser (PIL) and external pump-probe laser (PPL)] to the reference signal; (iii) the acceleration process in the LINAC, mainly noise in the rf power delivered to the accelerating sections as well as conversion of energy fluctuations of the e-bunch to timing jitter by the bunch compression (see e.g., [15]); and (iv) the uncertainty of the spike generation in the spontaneous undulator emission.

Once the FEL process has been initiated, the time of flight through the undulator chain and to the experimental chamber adds a negligible jitter and may only exhibit slow drifts due to temperature changes. In the seeded FEL scheme the third and fourth jitter sources listed above are canceled by the seeding process. Thus in a seeded FEL the timing jitter of the pump-probe experiment would be reduced to the sum of the timing errors of the seed and PPL lasers with respect to the reference, the relative jitter between the two links carrying the reference signal to the two lasers, and the jitter contribution of the optical transport of both beams to the point of interaction. At present, the first term is dominant and is expected to be on the order of a few tens of fs for the FERMI case. The

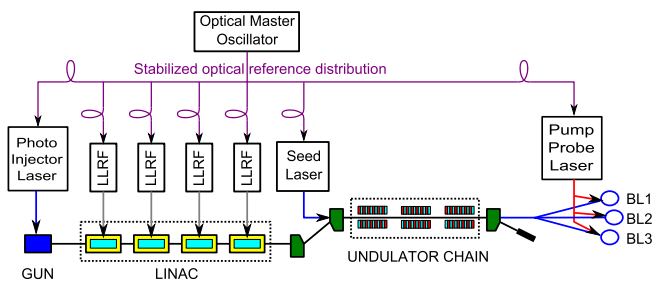


FIG. 1. Color scheme of a typical free electron laser. The electron bunch is generated in the rf photoinjector and accelerated in a linear accelerator, then compressed and fed to a chain of undulators. LLRF stands for low level rf electronics; BL1,2,3 are beam line experimental stations where FEL and external laser pulses are delivered.

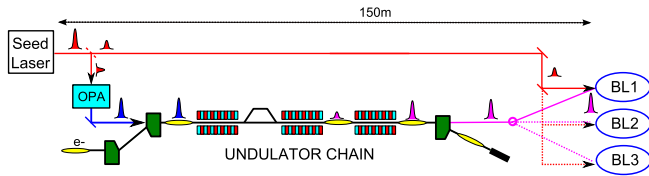


FIG. 2. Color sketch of the proposed scheme.

approach we propose here aims at further reducing this value by removing the dominant jitter contribution terms, namely the laser pulse-to-timing reference jitter. As it can be seen from Fig. 2 (only the layout after the LINAC is shown for simplicity), in the proposed scheme this is obtained by using a portion of the same laser pulse as a source for both seeding the FEL and as an external pump-probe pulse. The common initial laser pulse is a few mJ level near infrared laser pulse generated by a Ti:sapphire based amplifier. The pulse used for seeding the FEL (further referred to as SL) is shown in blue and has a deep UV wavelength in the case of FERMI. It is produced by the IR pulse through a chain of nonlinear processes [optical parametric amplifier (OPA) and harmonic generation] and sent to the undulators. The pulse shown in red (further referred to as PPL), is a portion of the same initial IR pulse which is sent through a dedicated optical transport to the beam line chamber for pump-probe experiments. The SL pulse meets the electron bunch (represented by the yellow ellipse) in the first undulator and initiates the FEL process. The FEL pulse propagates in the undulator chain and then through the x-ray beam transport optics, while the PPL pulse propagates through its transport in parallel and, if delay is properly chosen, arrives in the beam chamber simultaneously with the x-ray pulse. To take a full advantage of this scheme for reducing the pump-probe experiment jitter, it is important that the long beam transport of the PPL to the arrival point at the user stations does not introduce significant additional jitter. Further in this paper we show that with a properly designed optical transport this is indeed the case: the optical beam transport contribution to timing fluctuations can be kept much smaller than the above-mentioned dominant jitter contributions in the standard scheme.

To complete the picture, it should be said that for most of the FEL applications (photoinjector, seeding, pump-probe experiments), the local laser oscillator is typically a mode-locked (ML) femtosecond laser with a repetition rate in the 100 MHz range and pulse energy in the 1–10 nJ range. These pulses are subsequently amplified at reduced repetition rate in a regenerative and/or multipass amplifier to mJ range and used for harmonic conversion or OPA pumping. As a rule the repetition rate of the ML oscillator is locked to the reference timing signal by use of a PLL where the error signal is derived by rf mixing [16] and/or by an optical cross correlator [6] and the laser cavity length is controlled by coarse (motor based) and fine (piezo based)

actuators. Typically the ML lasers used are commercial Ti:sapphire based oscillators and even if advanced optical locking schemes are used, there is a residual phase noise resulting in a timing jitter in the 20–30 fs rms range (measured from 10 Hz to 1 MHz).

III. DESIGN OF THE OPTICAL BEAM TRANSPORT

The work described in this paper was driven by the need of setting up pump-probe experiments at the FERMI FEL and the idea for using the seed laser pulses for this purpose was born when the FEL construction has already been completed and the FEL was under commissioning. For this reason, the implementation of the scheme had to take into account the already existing infrastructure and some solutions that would have offered higher mechanical stability (like propagation of the beam underground in the undulator and experimental hall) were not feasible. The mechanical and optical design had to be adapted to the existing boundary conditions, while at the same time ensuring that the influence of acoustic noise and vibrations as well as slow thermally induced movements be minimized. In addition, to preserve the short pulse duration, dispersion and self-phase-modulation (SPM) effects needed to be minimized. For achieving these goals the following solutions were applied: (i) relay imaging for the beam propagation; (ii) minimization of the number of optical surfaces in transmission and their total thickness; (iii) large beam spot on all transmission optics so as to minimize the accumulated nonlinear phase; (iv) use of vacuum for the long straight part of beam propagation to avoid turbulence and nonlinear effects in air; and (v) insertion of a sufficient number of control points with diagnostics and actuators for fine beam steering to allow implementation of active beam stabilization.

A simplified optical scheme is shown in Fig. 3. We note that by necessity the beam trajectory contains seven beam-folding points at 45 degrees, where flat mirrors are used, for simplicity they are not shown on the scheme.

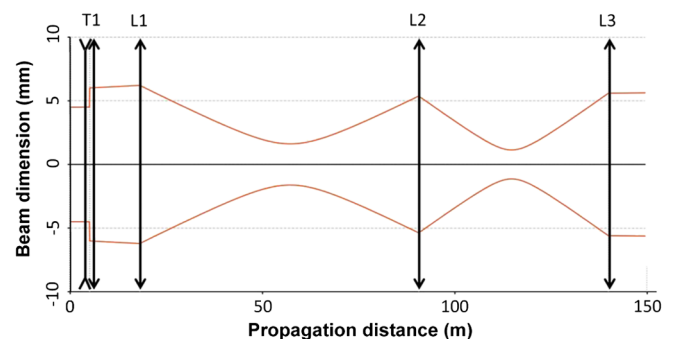


FIG. 3. Color dependence of spot size ($1/e^2$ diameter) versus distance of the IR beam during propagation from the seed laser table to the beam line stations, T1 is a telescope, L1,2,3 are long focal distance lenses. Beam folding mirrors are omitted.

The long straight part of the optical transport incorporates three long focal distance relay imaging lenses (L1–L3). The positions of the relay lenses could not be freely chosen and were decided on the basis of existing construction constraints, so the distances between them were 72.5 m (L1–L2) and 49.3 m (L2–L3) with lens focal distances of $L1 = 37.6$ m, $L2 = 15.0$ m and $L3 = 24.2$ m. There was the need to have a degree of freedom to match these values with the desired beam propagation mode; it was found that the best way to achieve it was the insertion of the telescope T1 (magnification 1.3) situated 13 m in front of the lens L1, permitting to vary the divergence of the beam entering the relay imaging part.

A ZEMAX ray tracing showed that the beam spot obtained in this way was small enough everywhere to avoid diffraction losses on the beam apertures (limited to about 48 mm) and was large enough on the lenses and windows (everywhere above 7 mm $1/e^2$ diameter) to keep SPM at a negligible level. This was confirmed by monitoring that the optical spectrum of the input pulse (12 nm bandwidth at 785 nm, up to 1 mJ at present) remained nearly unchanged at the beam transport exit.

When the FEL is operated, the IR pulse exiting the Ti: sapphire amplifier is weakly chirped (using its internal compressor) to optimize the OPA performance and has a duration of about 100 fs. The fraction of the pulse used as PPL travels through a total optical material of about 70 mm fused silica before arriving at the pump-probe stations, which introduces a second order dispersion and a third order dispersion of about 2600 fs² and 1900 fs³, respectively. As a result, the final pulse is positively chirped and has duration of about 140 fs. It can be compressed back to the 100 fs range at each pump-probe station by the use of a compact transmission grating based pulse compressor to be installed during the next FEL shutdown.

IV. ACTIVE POINTING STABILIZATION

The use of the transported beam for pump-probe experiments implies that it has to arrive in the interaction region with a very high pointing and timing stability. No matter how stable and well isolated the optical components used for the beam transport are, they will always exhibit small movements due to coupling of vibrations from the environment (typically rather noisy in this type of facility) and due to deformations induced by slow temperature changes, so the beam trajectory will not be perfectly constant. In addition, the laser beam exiting the amplifier has by itself a pointing instability, typically on the order of several microradians. It was clear therefore that to reach the goal of this work there was the necessity to implement an active beam pointing stabilization system. The latter was based on the introduction of a number of monitoring points and the implementation of high finesse actuators. In a complicated beam trajectory like in our case (the beam propagated in two rooms, in a part of the undulator hall tunnel and then in

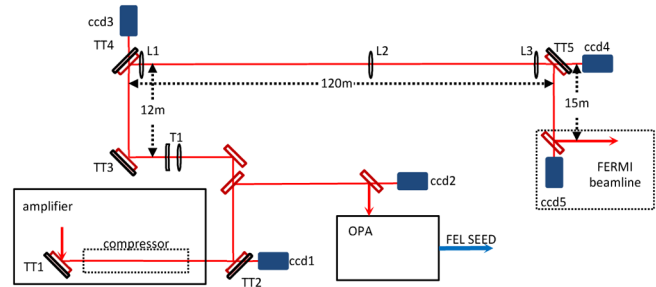


FIG. 4. Color layout of the optical beam stabilization, CCD1–CCD5 are Basler Scout or Ace cameras for transverse beam position diagnostics, TT1–TT5 are piezo tip-tilt mounts for two-axis fine beam steering.

a large part of the experimental hall) it is impossible to control the beam position on every mirror. Figure 4 shows a simplified scheme (not in scale) of the solution we implemented.

The first two control points are introduced in order to stabilize the pointing of the beam exiting the regenerative amplifier and are monitored by CCD1 and CCD2, the beam position on them is kept constant by piezo-driven tip-tilt mounts (TT1 and TT2). Given that the beam position on the mirror attached to TT1 was found to be rather stable without stabilization, the fine control of the beam position on CCD1 by TT1 stabilizes also the trajectory inside the pulse compressor and therefore allows one to keep the pulse length constant. The part of the beam sent to the beam transport is then monitored on CCD3 (entrance in the undulator hall) and CCD4 (at the end of the long straight section), and the beam position adjustment is based on TT3 and TT4. The last part of the transport, from the common distribution point to each FERMI beam line (here for simplicity we show only one, DiProi) is monitored by CCD5 and CCD6 (looking at the virtual sample position in the beam line chamber) and the fine beam steering is actuated by TT5 and TT6.

The maximum monitoring bandwidth of this CCD-based version of the feedback system is 50 Hz. The repetition rate of the amplified laser pulses is currently adjusted to 10 Hz to match the presently used LINAC repetition rate and will be set to 50 Hz in the future. For what concerns the bandwidth of the beam position steering, the limit on the side of the tip-tilt actuators (PI S-330.20L) is set by the relatively heavy mirrors to about 2 kHz, while the limit on the side of the controller, which is typically lower for commercial controllers, has been overcome in our case by utilizing home developed controller based on the Beagle-bone platform and has been shown to exceed 3 kHz [17].

To give an idea about the stability of the optical transport and the effect of the beam stabilization below we present some typical results. In Fig. 5 a typical beam image on CCD5 is presented, while the time behavior of the beam centroid horizontal and vertical position is shown

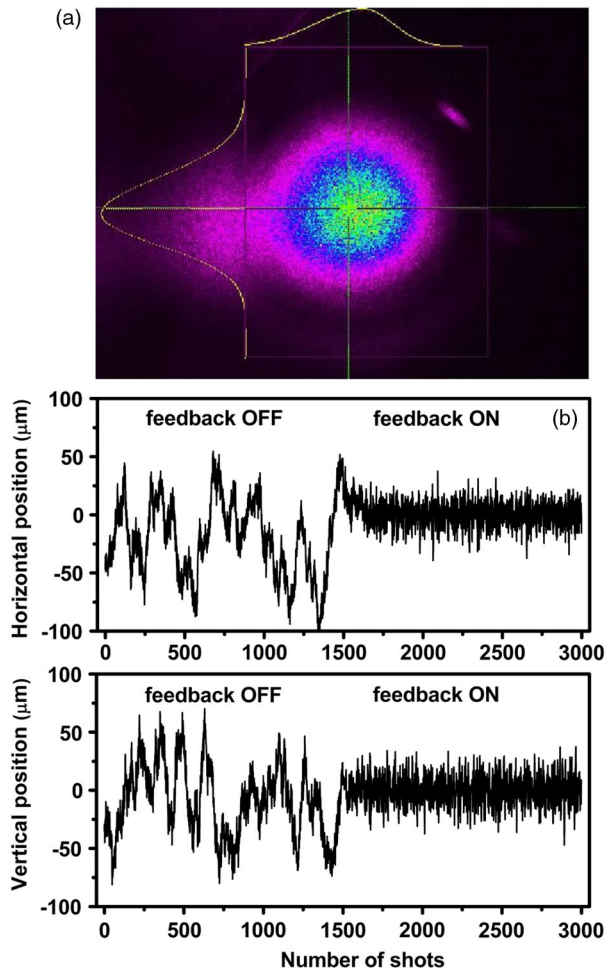


FIG. 5. (a) Color beam image on CCD5. (b) Horizontal (upper trace) and vertical beam centroid position recorded for each shot with feedback OFF (first 1500 shots) and after turning ON the feedback.

on Fig. 5(b), with feedback OFF (the first 1500 shots) and feedback ON (the next 1500 shots). The weak ghost image seen to the left of the main beam on Fig. 5(a) is caused by a reflection on the second surface of a folding mirror in front of CCD5 (not shown on the figure) and does not propagate to the user stations. Figure 5(b) shows that even with the feedback OFF the beam position after 150 m of propagation exhibits slow fluctuations of less than $40 \mu\text{m}$ rms. Turning ON the feedback allows the complete suppression of the oscillations with period higher than about 1 s (determined by the bandwidth of the feedback) and the shot-to-shot jitter is kept below $10 \mu\text{m}$ rms.

V. MEASUREMENT OF THE TIMING JITTER AND DRIFTS

The evaluation of the timing jitter of the transported PPL beam can be done in two ways. From a user point of view, the preferred modality would be a pump-probe measurement of an ultrafast process having well-defined time

structure done with the FEL pulse and the transported seed pulse. Measurements of this type have been recently performed in collaboration with FERMI users and will be reported in the near future; they indicated very good performance (10 fs level jitter with feedbacks ON). However, the information obtained in this way gives just the overall jitter and is not sufficient to state what the amount of jitter coming from different contributors is. For this reason here we present dedicated measurements and data which allow evaluating separately the performance of the beam transport as well as of the amplifiers on the seed laser table. The layout developed for this purpose is based on three different optical cross correlators (see Fig. 6). The reference pulse in all cases is derived from the mode-locked (ML) Ti:sapphire laser oscillator (Micra, Coherent) which is repetition rate locked to the reference timing pulses distributed over the facility. More details on the repetition rate locking can be found in [18]; here we will only mention that the error signal is derived by a balanced optical cross correlator (BOCC) and delivered to a home-built timing unit which drives the actuators controlling the cavity length. The main part of the laser oscillator output seeds a chirped-pulse regenerative amplifier followed by a single pass amplifier, which delivers 100 fs range pulses with up to 7 mJ of energy per pulse. As it is known, due to the long effective path in the regenerative amplifier, the amplified pulses typically exhibit temporal drifts that may exceed few hundred fs [19] and could obviously be a problem for obtaining stable seeded FEL operation. So, as a first step of our work an active compensation of these drifts has been implemented. The scheme involves first a real time measurement of the drift by a single shot cross correlator (SSCC1) which is set as follows. Small fractions of the amplified pulse and of the ML oscillator pulse enter a β -barium borate (BBO) crystal at a relative angle of 15 deg and the produced sum-frequency signal centered at 392 nm is imaged onto a CCD camera. Due to the beam tilt the relative arrival time of the two pulses is mapped in the position of the peak of the SFG signal in the horizontal plane [20,21]. The dependence of pulse delay versus

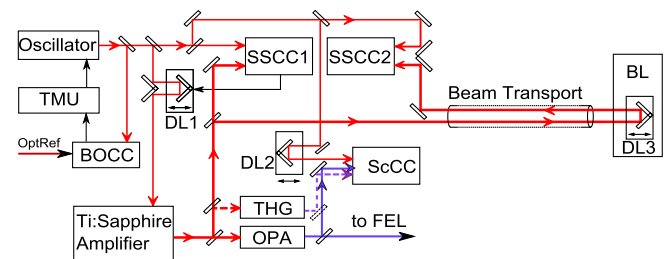


FIG. 6. Arrangement of the cross correlators for the jitter measurements described in the text. BOCC stands for balanced cross correlator, ScCC—a scanning cross correlator; SSC1 and SSC2—single shot cross correlators; BL—beam line chamber; DL1, DL2 and DL3—delay lines.

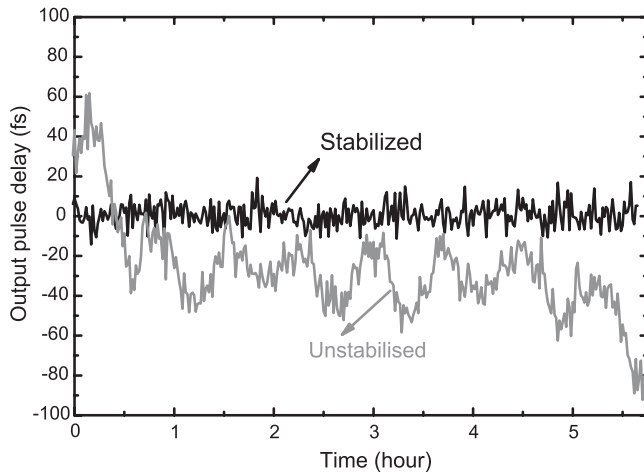


FIG. 7. Traces showing the timing fluctuations of the output pulse from the Ti:sapphire amplifier, measured by SSCC1; gray line: unstabilized; black line: active stabilization ON.

position allows a relative time shift detection sensitivity of better than 10 fs. A typical dependence of the pulse drift in about six hours measured in this way is shown by the red curve on Fig. 7. Parallel measurements of the laser room temperature (stabilized to about ± 0.25 deg) indicated that the temperature fluctuations are indeed the main factor for the observed slow timing fluctuations. To cancel them, we used the image centroid position of the CCD as an error signal for a feedback loop, acting on a high precision piezo-driven translation stage (DL1 on Fig. 6) which changes the delay of the oscillator pulse seeding the regenerative amplifier. When the feedback is turned ON the drift can be removed, as it is seen by the pulse position measurement for another six-hours period made with feedback ON shown by the black curve on Fig. 7. The remaining fast centroid instability along the horizontal axis is on the order of 6 fs is not compensated by this feedback due to its insufficient bandwidth (≤ 1 Hz). It is important to note that while this stabilization is essential for achieving stable seeded FEL operation, it does not modify the jitter/drift performance of the pump-probe scheme proposed in this paper because the regenerative amplifier is situated before the pulse splitting to SL and PPL part and therefore the time changes are canceled.

As it can be seen on the layout shown on Fig. 6, the part of the beam used to seed the FEL (about 70% of the energy of the Ti:sapphire amplifier) is used to pump an optical parametric amplifier (OPA). The latter is based on a commercial Opera-Solo traveling-wave parametric amplifier with signal and idler in the infrared (1.08 to 2.6 μm), where after a sequence of nonlinear mixing and harmonic generation the desired UV wavelength (typically in the 230–260 nm range) is produced. More details can be found in [22].

It is known that the OPA itself can be a source of non-negligible timing jitter and drift [23]. Considering that in

our setup only the pulses used to seed the FEL are generated by the OPA, it was important to evaluate the fluctuation of the pulses exiting the latter. For this purpose we used the scanning cross correlator which normally measures the pulse duration of the UV seed pulse (ScCC on Fig. 6) by performing collinear frequency mixing (difference frequency generation, DFG) of the UV pulse and a portion of the laser oscillator pulse in a BBO crystal. The DFG signal, which is in the 325–390 nm range, is detected at each shot by a photodiode with a current reading by a pico-ammeter AH 401B [24]. A plot of typical cross-correlation scan used for the calibration is shown in Fig. 8(a). In this case the jitter is measured by setting the delay to the middle of one of the slopes of the cross-correlation curve, recording its intensity fluctuations and then converting them to time fluctuations on the basis of the calibrated slope. The result of a measurement over 3000 shots is plotted in Fig. 8(b). The intensity fluctuations of the cross-correlated pulses were below 1.5% rms and 0.5% rms for the UV and IR pulses, respectively, so their contribution to the measured cross-correlation signal intensity fluctuations would correspond to below 2 fs and have been neglected here. The rms jitter value of 9.1 fs measured in this way was confirmed by several consecutive measurements so we take 9 fs to be a representative number for the typical total jitter introduced by the sequence Ti:sapphire amplifier—OPA. As a cross-check of our measurement setups, we performed the same collinear cross-correlation measurement also in a version where the UV OPA pulses were replaced by the UV pulses produced through third harmonic generation by the IR pulses exiting the amplifier (shown by the dashed line on Fig. 6) and the obtained results confirmed the jitter value of about 6 fs measured by the single shot cross correlator SSCC1 presented above in this paragraph. At this point, subtracting in quadrature the regenerative amplifier contribution we can estimate the net contribution of the OPA to the timing jitter between the IR pulse coming directly from the Ti:sapphire amplifier and the UV seed pulse generated by the OPA to be of about 6.7 fs rms.

The next step is the measurement of the timing fluctuations introduced by the 150 m long beam transport of the

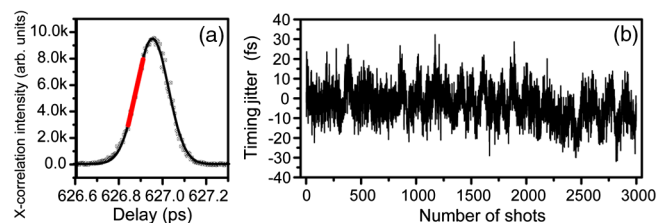


FIG. 8. (a) Color cross-correlation trace of the UV OPA pulse taken with ScCC, the slope of the red thick line is used for the intensity-to-time calibration. (b) A typical intensity vs time dependence where the vertical axis is already converted in time jitter.

pulse from the seed laser table to the user chamber for pump-probe measurements.

As can be seen on Fig. 6, this measurement is also based on a single-shot cross correlation (SSCC2). After arrival at the pump-probe station the pulse is reflected and sent back to the seed laser table, where it is cross correlated with a pulse emitted from the ultrafast oscillator. The total time of flight for propagation to the station in the experimental hall and back to the seed laser room for the IR laser beam is about $1 \mu\text{s}$, i.e., the oscillator pulse used for the cross correlation is emitted about $1.1 \mu\text{s}$ later than the oscillator pulse seeding the regenerative amplifier. It is well known (and confirmed by independent phase-noise measurements we made) that for such a short time interval the timing jitter of a repetition rate locked oscillator of the type we use is negligible, therefore the temporal stability of the transported back IR pulse measured by this cross correlation is a direct measurement of the timing jitter introduced by the sequence Ti:sapphire amplifier and optical beam transport. The sensitivity of the measurement is increased by a factor of 2 because of the double pass through the same optical path (we can safely assume that during the transit time of $1 \mu\text{s}$ all optical components can be considered “frozen”). A typical image of the sum-frequency signal at 392 nm is shown in Fig. 9(a), the two infrared beams (and therefore their pulse fronts) are tilted in the horizontal plane. The cross correlator was calibrated by measuring the image position shift in the horizontal plane after applying known time steps by the delay line. Then, the dependence of the centroid position was monitored for periods of a few thousand shots. For longer periods the measurement was influenced by slow timing drifts, typically of the order of up to 100–200 fs in 1 hour time scale. In Fig. 9(b) we show a

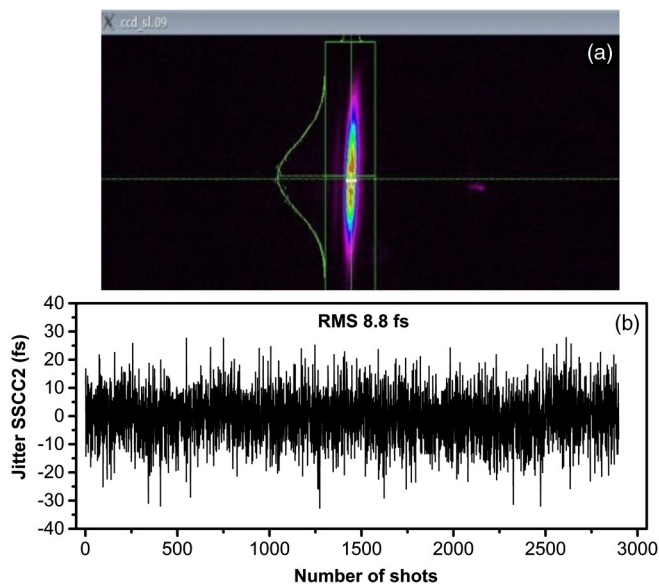


FIG. 9. (a) Color signal image from SSCC2. (b) A jitter measurement of 2900 consecutive pulses.

typical trace where the intensity fluctuation has been converted into time based on the above-mentioned calibration, the analysis of this trace indicates a Gaussian distribution with an rms value of 8.8 fs; other scans performed during the same day confirmed this value within ± 0.2 fs. Recalling that the rms jitter contribution of the Ti:sapphire amplifier was measured to be about 6 fs, we can state with a high degree of confidence that the double-pass timing jitter introduced by the optical beam transport from the seed laser table to the user station is only about 6.4 fs rms, and the single pass one, i.e., the contribution to the overall jitter in a pump-probe measurement which uses the transported pulse would be of about 3.2 fs rms over a few minutes of measuring time. The total jitter contribution of the laser part in a pump-probe measurement in our scheme, as presented on Fig. 2, would then be given by the sum (in quadrature) of the beam transport and the OPA contribution, and based on our measurements is estimated not to exceed a conservative value of 8 fs. In good agreement with this statement, the first pump-probe measurements of transient reflectivity on semiconductor samples performed recently on both DiProi and TIMEX FERMI beam lines demonstrated that the overall timing jitter between the IR pulse and the FEL is below 10 fs rms over tens of minutes (note that this latter value includes also the contribution of instabilities of the chamber, sample holder, etc.). A not less important finding was that the pump-probe measurement with the FEL confirmed our expectations that, thanks to the fact that over the long part of the beam transport the PPL pulse and the FEL pulse propagate in parallel in the same temperature environment, the relative path-length drifts were very small and the “zero” time of the measurement stayed constant without need of correction in several tens of minutes time scale. We note that in the case of pump-probe measurements which last longer and need the slow timing drift of the optical transport to be precisely compensated, this can be done in a relatively straightforward way: a small portion of the transported beam can be reflected back and used to operate SSCC2 online. This will allow one to implement a feedback similar to the one compensating the timing drift of the regenerative amplifier and described in the beginning of this chapter (see Fig. 7 and related text).

VI. CONCLUSIONS

The work described here was motivated by the need to provide a reliable solution for performing pump-probe measurements at the FERMI FEL experimental stations. This was done by a free-space transport of ultrashort pulses generated by the FERMI seed laser situated about 150 m away. The obtained results satisfy this main goal and demonstrate that a careful optical and mechanical design, combined with the implementation of high-performance transverse beam-position feedbacks, allows one to transport ultrashort laser pulses at such a distance keeping the added timing jitter very low (on the 3 fs level). Even lower values

(and therefore even subcycle pulse arrival time stability at 800 nm over minutes) can be expected if pulses at higher repetition rates allowing the implementation of higher bandwidth feedbacks, are used. We note that this could for example be easily done in our case by using the native 1 kHz repetition rate of the Ti:sapphire amplifier and position sensitive detectors instead of CCD cameras.

The pulses transported to the FERMI beam lines are now available for user experiments and first results have already been obtained and will soon be reported. We believe our technique adds one more argument for using the seeding scheme and expect it could be successfully implemented also at other FEL facilities. While the motivation of this work was the application to FELs, we think the demonstrated results are of interest for a broader community working on ultrafast laser applications, and more specifically on ultrafast experiments at large scale facilities like different accelerator types, synchrotrons, large laser facilities, phased-array antennas, etc.

ACKNOWLEDGMENTS

This work was performed in the framework of the FERMI project of Elettra-Sincrotrone Trieste, and partially supported by the Italian Ministry of Education, Universities and Research (MIUR) under Grants FIRB-RBAP06AWK3 and ELI. We thank G. Loda for designing the custom mechanics supports for the beam transport.

-
- [1] P. Emma, R. Akre, J. Arthur, R. Bionta, C. Bostedt, J. Bozek, A. Brachmann, P. Bucksbaum, R. Coffee, F.-J. Decker *et al.*, *Nat. Photonics* **4**, 641 (2010).
 - [2] B. W. J. McNeil and R. Thompson, *Nat. Photonics* **4**, 814 (2010).
 - [3] S. Tanaka and S. Mukamel, *J. Chem. Phys.* **116**, 1877 (2002).
 - [4] F. Bencivenga, S. Baroni, C. Carbone, M. Chergui, M. B. Danailov, G. De Ninno, M. Kiskinova, L. Raimondi, C. Svetina, and C. Masciovecchio, *New J. Phys.* **15**, 123023 (2013).
 - [5] R. K. Shelton, S. M. Foreman, L. S. Ma, J. L. Hall, H. C. Kapteyn, M. M. Murnane, M. Notcutt, and J. Ye, *Opt. Lett.* **27**, 312 (2002).
 - [6] A. Bartels, S. A. Diddams, T. M. Ramond, and L. Hollberg, *Opt. Lett.* **28**, 663 (2003).
 - [7] M. Beye, O. Krupin, G. Hays, A. H. Reid, D. Rupp, S. de Jong, S. Lee, W.-S. Lee, Y.-D. Chuang, R. Coffee, A. Föhlisch *et al.*, *Appl. Phys. Lett.* **100**, 121108 (2012).
 - [8] R. Riedel, A. Al-Shemmary, M. Gensch, T. Golz, M. Harmand, N. Medvedev, M. J. Prandolini, K. Sokolowski-Tinten, S. Toleikis, U. Wegner, B. Ziaja, N. Stojanovic, and F. Tavella, *Nat. Commun.* **4**, 1731 (2013).
 - [9] S. Schulz, M. K. Czwalińska, M. Felber, P. Prędki, S. Schefer, H. Schlarb, and U. Wegner, *Proc. SPIE Int. Soc. Opt. Eng.* **8778**, 87780R (2013).
 - [10] M. Harmand, R. Coffee, M. R. Bionta, M. Chollet, D. French, D. Zhu, D. M. Fritz, H. T. Lemke, N. Medvedev, B. Ziaja, S. Toleikis, and M. Cammarata, *Nat. Photonics* **7**, 215 (2013).
 - [11] E. Allaria, R. Appio, L. Badano, W. A. Barletta, S. Bassanese, S. G. Biedron, A. Borga, E. Busetto, D. Castronovo, P. Cinquegrana *et al.*, *Nat. Photonics* **6**, 699 (2012).
 - [12] E. Allaria, D. Castronovo, P. Cinquegrana, P. Craievich, M. Dal Forno, M. B. Danailov, G. D’Auria, A. Demidovich, G. De Ninno, S. Di Mitri *et al.*, *Nat. Photonics* **7**, 913 (2013).
 - [13] L. H. Yu, *Phys. Rev. A* **44**, 5178 (1991).
 - [14] T. Togashi, E. J. Takahashi, K. Midorikawa, M. Aoyama, K. Yamakawa, T. Sato, A. Iwasaki, S. Owada, T. Okino, K. Yamanouchi *et al.*, *Opt. Express* **19**, 317 (2011).
 - [15] P. Craievich, S. Di Mitri, M. Milloch, G. Penco, and F. Rossi, *Phys. Rev. ST Accel. Beams* **16**, 090401 (2013).
 - [16] M. J. W. Rodwell, K. J. Weingarten, D. M. Bloom, T. Baer, and B. H. Kolner, *Opt. Lett.* **11**, 638 (1986).
 - [17] S. Cleva, L. Pivetta, and P. Sigalotti, in *Proceedings of ICALEPCS2013, San Francisco, CA, USA*, p. 464.
 - [18] P. Sigalotti, P. Cinquegrana, A. Demidovich, R. Ivanov, I. Nikolov, G. Kurdi, and M. B. Danailov, *Proc. SPIE Int. Soc. Opt. Eng.* **8778**, 87780Q (2013).
 - [19] S. Klingebiel, I. Ahmad, C. Wandt, C. Skrobol, S. A. Trushin, Z. Major, F. Krausz, and S. Karsch, *Opt. Express* **20**, 3443 (2012).
 - [20] J. Jansky, G. Corradi, and R. N. Gyuzalian, *Opt. Commun.* **23**, 293 (1977).
 - [21] R. Trebino, *Frequency Resolved Optical Gating: The Measurement of Ultrashort Laser Pulses* (Kluwer Academic Publishers, Boston, MA, 2002), Chap. 7.
 - [22] M. B. Danailov, P. Cinquegrana, A. A. Demidovich, R. Ivanov, I. Nikolov, and P. Sigalotti, in *Proceedings of 33rd International FEL Conference 2011 Shanghai, China, 2011, SINAP 2012*, p. 183.
 - [23] A. Schwarz, M. Ueffing, Y. Deng, X. Gu, H. Fattahi, T. Metzger, M. Ossiander, F. Krausz, and R. Kienberger, *Opt. Express* **20**, 5557 (2012).
 - [24] The device is produced by the Elettra Instrumentation and Detectors Laboratory; information can be found on <http://www.elettra.trieste.it/lightsources/labs-and-services/instrumentation-and-detectors-lab/products.html>.